PNAS RESEARCH ARTICLE | PSYCHOLOGICAL AND COGNITIVE SCIENCES

Attention control ability is associated with frontoparietal control network interactions

Dolly T. Seeburger[a,1], Jason S. Tsukahara[b], Nan Xu[c], Vishwadeep Ahluwalia[d], Shella D. Keilholz[e], and Randall W. Engle[a,1]

Affiliations are included on p. 7.

Contributed by Randall W. Engle; received September 24, 2025; accepted March 31, 2026; reviewed by B. J. Casey and Aaron Kucyi

Attention control predicts academic achievement, professional success, and health outcomes. However, the neural basis of stable, individual differences in attention control remains unclear. Prior research has emphasized momentary fluctuations in attentional engagement, often overlooking enduring individual differences. Here, we applied the quasi-periodic pattern analysis of infraslow functional magnetic resonance imaging (fMRI) dynamics in a large sample (N = 196) to test whether trait attention control is reflected in network-level brain activity as well as the locus coeruleus (LC). Using latent-variable measures of attention control, working memory capacity, and fluid intelligence, we isolated the unique contribution of attention control across rest, 1-back, and 3-back conditions. As cognitive demand increased, individuals with higher attention control exhibited more coordinated activity of the frontoparietal control network (FPCN): they showed enhanced coupling with the dorsal attention network (DAN), and greater engagement with the LC and stronger decoupling from the default mode network (DMN). Even at rest, high attention individuals demonstrated stronger FPCN–DAN coupling and little to no correlation between FPCN–DMN, indicating that attentional capacity is reflected in both task-evoked reconfiguration and baseline network architecture. These findings reveal how attention control, as an ability, is instantiated in the brain's dynamic architecture.

attention control | individual differences | brain networks | locus coeruleus | fMRI

Significance

Attention control is fundamental to human cognition, and people differ in this trait to maintain focus. These individual differences shape success in school, work, and health, but their neural basis remains unclear. Our study shows that attention control is reflected in the brain's dynamic interaction. Individuals higher in attention control demonstrated more coordination between the frontoparietal control network with other attention networks, as well as the locus coeruleus, a major neuromodulatory hub. Remarkably, these signatures are present even in the absence of cognitive load. These findings demonstrate that attention control is not just momentary fluctuations, but a stable trait embedded in large-scale brain dynamics, providing a framework for understanding the neural organization of individual differences.

Why Attention Control Matters. Attention control refers to the domain-general ability to focus on goal-relevant information while resisting distraction and interference from task-irrelevant thoughts and events (1, 2). It is an ability that has been described as "Supervisory Attentional System" (3), "cognitive control" (4, 5), "executive function" (6), "executive control" (7), "executive attention" (8, 9), and the "central executive" (10). This ability can manifest at both the trait level—a relatively stable individual difference—and the state level, where the ability can be diminished due to external distractions and even internal challenges such as fatigue, sleep deprivation, and emotional stress. As a trait variable, it can predict achievements in academics (11–14), is correlated with mental and physical health (15), and has positive effects on social and psychological development (16). In adults, it is linked to job performance (17). Despite its broad relevance, the neural basis of stable, trait-level differences in attention control remains poorly understood.

Gaps in Prior Work and Candidate Systems. Existing research provides insight into how the average brain responds to fluctuating attentional demands (i.e., state-level variation), however, much less is known about how these responses vary between individuals (i.e., trait-level differences) as well as the interaction between the two factors. Research on individual differences in attention control has largely taken two approaches (18). Some studies link brain activity during tasks to behavior measured concurrently. In contrast, many trait-level studies focus on resting-state networks, with little attention to how these networks engage during tasks or shift from rest to task (19–24). Bridging these approaches may help clarify how trait-level differences in attention control are reflected in the dynamic engagement of brain networks from rest to task. This gap in knowledge limits our understanding of the true neural basis of individual differences in attention control and constrains the identification of brain-based biomarkers for attention-related disorders. Fortunately, many recent studies have moved toward an approach that bridges this gap (25, 26). Evidence converges on the prefrontal cortex (PFC) (27) as a central node for maintaining task goals. Thus, it has been proposed that individual differences in attention control are likely mediated by the PFC, particularly the dorsolateral PFC (dlPFC) (28). Yet, control is unlikely to be localized to a single region. The frontoparietal control network (FPCN) is a distributed hub that encompasses the dorsolateral and rostrolateral PFC along with areas of the posterior parietal cortex (PPC) including the inferior (IPL) and

Author contributions: D.T.S., J.S.T., and R.W.E. designed research; D.T.S., J.S.T., N.X., and V.A. performed research; S.D.K. contributed new reagents/analytic tools; D.T.S., J.S.T., N.X., and V.A. analyzed data; J.S.T., N.X., and V.A. revised the paper; S.D.K. provided method; R.W.E. provided methodology; and D.T.S. wrote the paper.

Reviewers: B.J.C., Barnard College; and A.K., Drexel University.

The authors declare no competing interest.

[1]To whom correspondence may be addressed. Email: dseeburger3@gatech.edu or randall.engle@gatech.edu.

This article contains supporting information online at https://www.pnas.org/lookup/suppl/doi:10.1073/pnas.2526828123/-/DCSupplemental.

Published May 4, 2026.

superior parietal lobule (SPL). It is supported by its connectivity with other networks (29–32), including the default mode network (DMN) (33, 34) involved in internally oriented thought, the dorsal attention network (DAN) (29) which supports externally oriented attention, and the ventral attention network (VAN) (35, 36) which activates during salience detection. Due to its highly connected (37, 38) architecture, the FPCN is the prime candidate to play a central role in coordinating information processing across the brain as a unitary domain general system regulating top–down attention control. Spreng et al. (39) concluded that the FPCN works as a cortical mediator between DAN and DMN by flexibly coupling with one or the other according to task demands. We push this framework further by predicting that this relationship is also mediated by individual differences in attention control.

Another important consideration is that the FPCN maintains reciprocal anatomical connections with the locus coeruleus (LC) (40), the brain's primary source of norepinephrine. Through this neuromodulatory system, the LC–NE system plays a central role in regulating arousal and shaping large-scale brain network dynamics. In particular, the LC shares strong reciprocal anatomical and functional connections with the dorsal anterior cingulate cortex (dACC)—a principal hub of the FPCN—forming an integrative circuit that links cortical control systems with ascending neuromodulatory input (41, 42). Phasic LC activity is thought to promote coordinated engagement and reconfiguration of large-scale brain networks during cognitively demanding states (43, 44). Individual differences in how effectively LC-mediated neuromodulatory signals coordinate these network dynamics may therefore contribute to trait-level variation in attention control (45, 46).

QPP Framework and the Present Study. A promising tool for capturing the dynamics of large-scale networks is the quasi-periodic pattern (QPP) (47, 48) analysis, which identifies recurring, infraslow spatiotemporal patterns of brain activity. This measure also preserves temporal information and has been shown to account for substantial variance (49) in fMRI signals.

QPPs reveal robust anticorrelations between the DMN and DAN that have been observed at rest (33, 50) and are also linked to task performance (51–54). Weaker anticorrelation has been reported in ADHD patients (55). Moreover, the QPP signatures are shown to be stable within individuals across days (56), raising the possibility that they may index trait-level differences. Yet no study has directly tested whether infraslow network dynamics track stable attentional differences or how these interactions evolve with increasing cognitive demand.

We addressed this gap by combining a large sample (N = 196), latent-variable modeling of attention control, working memory, and fluid intelligence constructs, with the QPP analysis across rest, 1-back, and 3-back tasks. Participants first completed a battery of computerized tasks to measure cognitive constructs (*SI Appendix*, Table S2) across two separate days. They then returned for a single fMRI session, during which they completed n-back tasks and a resting-state scan. For more information refer to the Methods and Materials section as well as *SI Appendix*.

This design allowed us to isolate the unique contribution of attention control to brain network dynamics and connect trait-level with state-level interactions. We hypothesized that the synchrony of the FPCN with other large-scale networks (DMN, DAN, and VAN), as well as with the LC, would reflect differences in trait-level attention control, and that these differences would become more pronounced under increased task demands.

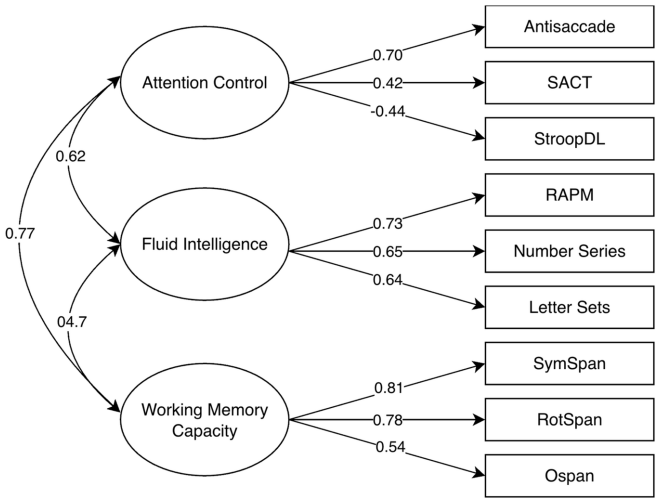

Fig. 1. Three-factor model using confirmatory factory analysis to capture trait-level attention control, fluid intelligence, and working memory capacity, $\chi^2(196) = 39.93$, $P < 0.05$, CFI = 0.96, RMSEA = 0.06 [0.02, 0.09]. All factor loadings are significant ($P < 0.001$). *SACT* Sustained Attention to Cue Task, *StroopDL* Stroop task with an adaptive response deadline, *RAPM* Raven's Advanced Progressive, *SymSpan* Symmetry Span, *OSpan* Operation Span, *RotSpan* Rotation Span.

Results

Latent-Variable Modeling of Cognitive Constructs. We first validated the measurement model for attention control, working memory capacity, and fluid intelligence. A three-factor confirmatory factor analysis showed a good fit, $\chi^2(24) = 39.93$, $P < 0.05$, CFI = 0.96, RMSEA = 0.06 [0.02, 0.09]. All factor loadings were significant ($P < 0.001$). As expected, the latent factors were highly correlated (r = 0.62 to 0.74) which is consistent with previous studies, known as the positive manifold (45–47); see Fig. 1. For that reason, to understand if the QPP is indeed capturing attention control, it is crucial to look at attention control's unique contribution. To do so, we removed the shared variance of fluid intelligence and working memory capacity and entered the residualized attention control score into the multilevel-model. Factor loadings and correlations are reported in *SI Appendix*, Tables S1 and S2.

d' was used to assess performance on the 1-back (Mean d' = 3.04, SD = 1.14) and 3-back (Mean d' = 1.57, SD = 0.73) tasks. The unresidualized attention control factor correlated with 1-back performance (r = 0.300, $P < 0.001$) and 3-back performance (r = 0.460, $P < 0.002$). However, the unique residualized attention control factor correlated only with the 1-back performance (r = 0.211, $P < 0.01$) and not 3-back performance (r = 0.079, $P > 0.05$).

FPCN and DMN Correlation. The FPCN–DMN correlation changed significantly with task demands, $F(2, 27{,}238) = 285.94$, $P < 0.001$, partial $\eta^2 = 0.021$, such that they were positively correlated at rest (β = 0.199, 99% CI [0.173, 0.224], SE = 0.01, $t(27{,}238) = 19.88$, $P < 0.001$), became less positively correlated during 1-back (β = 0.115, 99% CI [0.088, 0.142], SE = 0.01, $t(27{,}238) = 10.97$, $P < 0.001$), and were negatively correlated during 3-back (β = –0.139, 99% CI [–0.167, –0.112], SE = 0.01, $t(27{,}238) = -13.12$, $P < 0.001$). Significant changes were observed across all task pairs (rest vs. 1-back, $P < 0.001$; 1-back vs. 3-back, $P < 0.001$; rest vs. 3-back, $P < 0.001$).

Critically, this pattern interacted with attention control uniquely, $F(2, 27{,}238) = 14.91$, $P < 0.001$, partial $\eta^2 = 0.001$; see Fig. 2*A*. Higher attention control was associated with a less positive FPCN–DMN correlation during resting state ($\beta = -0.049$, 99% CI [–0.075, –0.023], $SE = 0.01$, $t(27{,}238) = -4.90$, $P < 0.001$). Individuals lower on attention control showed a greater decrease in the FPCN–DMN correlation from rest to 1-back ($\beta = 0.078$, 99% CI [0.040, 0.115], $SE = 0.02$, $t(27{,}238) = 5.37$, $P < 0.001$), as well as from rest to 3-back ($\beta = 0.050$, 99% CI [0.012, 0.087], $SE = 0.02$, $t(27{,}238) = 3.43$, $P < 0.001$). However, attention control was not related to change in FPCN–DMN correlation from 1-back to 3-back ($\beta = -0.028$, 99% CI [–0.066, 0.011], $SE = 0.02$, $t(27{,}238) = -4.90$, $P = 0.062$); that is, high and low attention control individuals showed the same magnitude of a switch from a positive FPCN–DMN correlation during 1-back to a negative FPCN–DMN correlation during 3-back.

After accounting for the shared variance between 1-back performance and attention control, neither 1-back performance ($\beta = 0.012$, 99% CI [–0.016, 0.040], $SE = 0.01$, $t(8{,}844) = 1.11$, $P = 0.268$) nor attention control ($\beta = 0.026$, 99% CI [–0.002, 0.054], $SE = 0.01$, $t(8{,}844) = 2.43$, $P = 0.015$) was associated with the FPCN–DMN correlation in the 1-back. After accounting for the shared variance between 3-back performance and attention control, neither 3-back performance ($\beta = 0.009$, 99% CI [–0.019, 0.038], $SE = 0.01$, $t(8{,}194) = 0.84$, $P = 0.399$) nor attention control ($\beta = -0.016$, 99% CI [–0.044, 0.013], $SE = 0.01$, $t(8{,}194) = -1.41$, $P = 0.160$) was related the FPCN–DMN correlation in the 3-back.

FPCN and DAN Correlation. The FPCN–DAN correlation changed significantly with task demands, $F(2, 27{,}238) = 651.65$, $P < 0.001$, partial $\eta^2 = 0.05$, such that they were slightly negatively correlated at rest ($\beta = -0.027$, 99% CI [–0.052, –0.002], $SE = 0.01$, $t(27{,}238) = -2.76$, $P = 0.006$), became positively correlated during 1-back ($\beta = 0.095$, 99% CI [0.069, 0.121], $SE = 0.01$, $t(27{,}238) = 9.30$, $P < 0.001$), and became more positively correlated during 3-back ($\beta = 0.470$, 99% CI [0.443, 0.496], $SE = 0.01$, $t(27{,}238) = 45.44$, $P < 0.001$). Significant changes were observed across all task pairs (rest vs. 1-back, $P < 0.001$; 1-back vs. 3-back, $P < 0.001$; rest vs. 3-back, $P < 0.001$).

Critically, this pattern interacted with attention control uniquely, $F(2, 27{,}238) = 37.21$, $P < 0.001$, partial $\eta^2 = 0.003$; see Fig. 2*B*. Higher attention control was associated with a less negative and slightly positive FPCN–DAN correlation during resting-state ($\beta = 0.054$, 99% CI [0.029, 0.079], $SE = 0.01$, $t(27{,}238) = 5.58$, $P < 0.001$). Individuals lower on attention control showed a greater shift to a more positive FPCN–DAN correlation from rest to 1-back ($\beta = -0.097$, 99% CI [–0.134, –0.061], $SE = 0.01$, $t(27{,}238) = -6.88$, $P < 0.001$), though not from rest to 3-back ($\beta = 0.019$, 99% CI [–0.018, 0.055], $SE = 0.01$, $t(27{,}238) = 1.33$, $P = 0.183$). Individuals higher on attention control showed a greater increase in the positive FPCN–DAN correlation from 1-back to 3-back ($\beta = 0.116$, 99% CI [0.079, 0.154], $SE = 0.02$, $t(27{,}238) = 7.99$, $P < 0.001$).

After accounting for the shared variance between 1-back performance and attention control, 1-back performance was

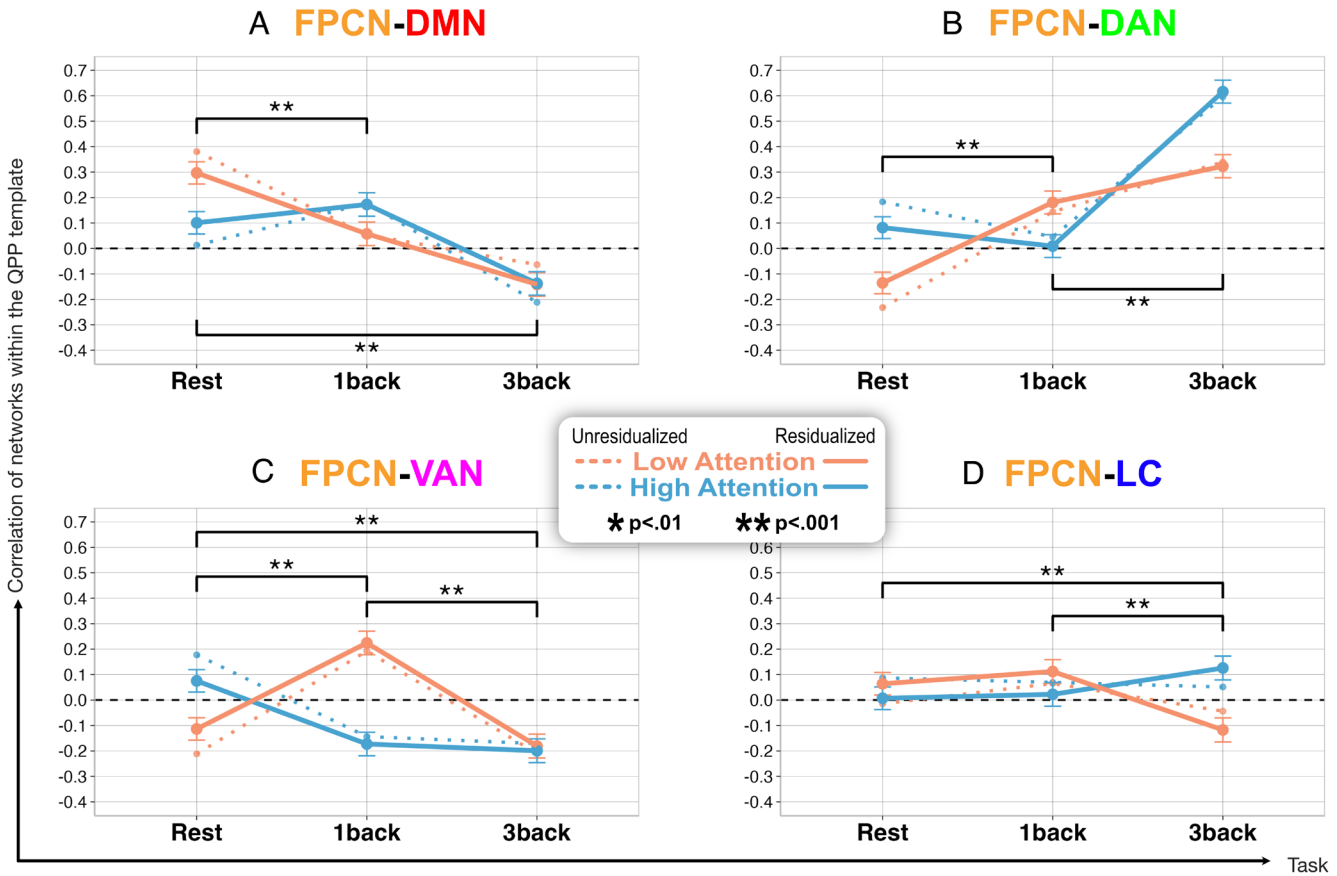

Fig. 2. Multilevel modeling results of trait-level attention control, task conditions, and the network correlations within the QPP template. (*A*) Correlation of the FPCN–DMN. (*B*) Correlation of the FPCN–DAN. (*C*) Correlation of the FPCN–VAN. (*D*) Correlation of the FPCN–LC within the QPP template. Results visualized as extreme groups with statistics on data from all subjects. High attention are individuals +2SD and low attention are individuals −2SD from the mean. Solid lines indicate unique contribution of attention control (residualized score), dotted lines indicate shared variance of attention control with working memory capacity and fluid intelligence (unresidualized score). *FPCN* frontoparietal control network, *DMN* default mode network, *DAN* dorsal attention network, *VAN* ventral attention network, *LC* locus coeruleus, *QPP* quasi-periodic pattern.

associated with a greater positive FPCN–DAN correlation in the 1-back (β = 0.031, 99% CI [0.003, 0.058], SE = 0.01, t(8,844) = 2.82, P = 0.005), however, attention control showed the opposite pattern as it was associated with less of a positive FPCN–DAN correlation in the 1-back (β = –0.049, 99% CI [–0.077, –0.021], SE = 0.01, t(8,844) = –4.55, P < 0.001). After accounting for the shared variance between 3-back performance and attention control, 3-back performance was not associated with the FPCN–DAN correlation in the 3-back (β = 0.016, 99% CI [–0.009, 0.042], SE = 0.01, t(8,194) = 1.63, P = 0.104), but attention control was associated with a greater positive correlation (β = 0.082, 99% CI [0.056, 0.107], SE = 0.01, t(8,194) = 8.27, P < 0.001). Nevertheless, when not accounting for differences in attention control 3-back performance was associated with a greater positive FPCN–DAN correlation (β = 0.030, 99% CI [0.005, 0.055], SE = 0.01, t(8,196) = 3.08, P = 0.002).

FPCN and VAN Correlation. The FPCN–VAN correlation changed significantly with task demands, F(2, 27,238) = 115.59, P < 0.001, partial η^2 = 0.008, such that they were slightly negative but nonsignificantly correlated at rest (β = –0.019, 99% CI [–0.045, 0.007], SE = 0.01, t(27,238) = –1.90, P = 0.057), became slightly positive but nonsignificantly correlated during 1-back (β = 0.026, 99% CI [–0.001, 0.053], SE = 0.01, t(27,238) = 2.45, P = 0.014), and became negatively correlated during 3-back (β = –0.190, 99% CI [–0.217, –0.163], SE = 0.01, t(27,238) = –17.81, P < 0.001). Significant changes were observed across all task pairs (rest vs. 1-back, P < 0.001; 1-back vs. 3-back, P < 0.001; rest vs. 3-back, P < 0.001).

Critically, this pattern interacted with attention control uniquely, F(2, 27,238) = 51.39, P < 0.001, partial η^2 = 0.004; see Fig. 2*C*. Higher attention control was associated with a less negative and slightly positive FPCN–VAN correlation during resting-state (β = 0.047, 99% CI [0.021, 0.073], SE = 0.01, t(27,238) = 4.70, P < 0.001). Higher and lower attention control individuals showed opposite patterns in the change from rest to 1-back (β = –0.146, 99% CI [–0.184, –0.109], SE = 0.02, t(27,238) = –10.05, P < 0.001); that is, higher attention control was associated with a shift to a more negative FPCN–VAN correlation and lower attention control was associated with a shift to a more positive FPCN–VAN correlation. Individuals higher on attention control showed more of a change to a greater negative FPCN–VAN correlation from rest to 3-back (β = –0.052, 99% CI [–0.090, –0.014], SE = 0.02, t(27,238) = –3.54, P < 0.001). Individuals lower on attention control showed more of a shift to a greater negative FPNC-VAN correlation from 1-back to 3-back (β = 0.095, 99% CI [0.056, 0.133], SE = 0.02, t(27,238) = 6.31, P < 0.001).

After accounting for the shared variance between 1-back performance and attention control, 1-back performance was associated with a greater positive FPCN–VAN correlation in the 1-back (β = 0.035, 99% CI [0.0007, 0.063], SE = 0.01, t(8,844) = 3.25, P = 0.001), however, attention control showed the opposite pattern as it was associated with a greater negative FPCN–VAN correlation in the 1-back (β = –0.106, 99% CI [–0.134, –0.079], SE = 0.01, t(8,844) = –9.84, P < 0.001). After accounting for the shared variance between 3-back performance and attention control, 3-back performance was associated with a less negative FPCN–VAN correlation in the 3-back (β = 0.054, 99% CI [0.026, 0.082], SE = 0.01, t(8,194) = 4.93, P < 0.001), however, attention control was not associated with the FPCN–VAN correlation in the 3-back (β = –0.024, 99% CI [–0.053, 0.004], SE = 0.01, t(8,194) = –2.22, P = 0.027).

FPCN and LC Correlation. The FPCN–LC correlation changed significantly with task demands, F(2, 27,238) = 8.71, P < 0.001, partial η^2 = 0.001, such that it was slightly positively correlated in rest (β = 0.036, 99% CI [0.009, 0.062], SE = 0.01, t(27,238) = 3.52, P < 0.001) and 1-back (β = 0.067, 99% CI [0.040, 0.095], SE = 0.01, t(27,238) = 6.34, P < 0.001), and was not correlated in 3-back (β = 0.004, 99% CI [–0.023, 0.032], SE = 0.01, t(27,238) = 0.40, P = 0.692). There was only a significant difference between 1-back and rest (P < 0.001).

Critically, this pattern interacted with attention control uniquely, F(2, 27,238) = 18.64, P < 0.001, partial η^2 = 0.001; see Fig. 2*D*. Attention control was not related to the FPCN–LC correlation at rest (β = –0.014, 99% CI [–0.040, 0.012], SE = 0.01, t(8, 194) = –1.41, P = 0.159) or during 1-back (β = –0.022, 99% CI [–0.050, 0.005], SE = 0.01, t(8, 194) = –2.11, P = 0.035); but it was during 3-back (β = 0.061, 99% CI [0.033, 0.088], SE = 0.01, t(27,238) = 5.67, P < 0.001). Higher attention control individuals showed a positive increase in the FPCN–LC correlation from rest to 3-back (β = 0.075, 99% CI [0.037, 0.113], SE = 0.02, t(27,238) = 5.09, P < 0.001) and 1-back to 3-back (β = 0.083, 99% CI [0.044, 0.122], SE = 0.02, t(27,238) = 5.51, P < 0.001), while lower attention control individuals showed a negative decrease. That is, the biggest difference related to attention control was when task demand was at its highest during 3-back, lower attention individuals' FPCN–LC were negatively correlated, while higher attention individuals' were positively correlated.

After accounting for the shared variance between 1-back performance and attention control, neither 1-back performance (β < –0.001, 99% CI [–0.029, 0.026], SE = 0.01, t(8,844) = –0.14, P = 0.890) nor attention control (β = –0.022, 99% CI [–0.050, 0.006], SE = 0.01, t(8,844) = –2.04, P = 0.042) was associated with the FPCN–LC correlation in the 1-back. After accounting for the shared variance between 3-back performance and attention control, 3-back performance was not associated with the FPCN–LC correlation in the 3-back (β = 0.018, 99% CI [–0.010, 0.047], SE = 0.01, t(8,194) = 1.65, P = 0.099), but attention control was associated with a greater positive correlation (β = 0.062, 99% CI [0.033, 0.091], SE = 0.01, t(8,194) = 5.53, P < 0.001). Nevertheless, when not accounting for differences in attention control 3-back performance was associated with a greater positive FPCN–LC correlation (β = 0.029, 99% CI [0.001, 0.058], SE = 0.01, t(8,196) = 2.64, P = 0.008).

Visualization of the QPP Templates. A visualization of the QPP templates using a high and low group split (n = 30) of the residualized attention control estimated scores confirms these multilevel modeling results; see Fig. 3.

Discussion

In line with the framework put forward by Spreng et al. (39), we demonstrated that the FPCN functions as a domain-general hub that couples with the DMN or the DAN depending on whether attention is internally or externally oriented (i.e., state-level). A key advancement made from this study is the clarification that these dynamics are not merely state-dependent but that they are also shaped by trait-level attention control.

Across analyses, attention control predicted systematic differences in how the FPCN reconfigured its coupling with other brain systems as cognitive demands increased. A consistent pattern emerged in which individuals with lower attention control showed larger connectivity changes between rest and the low-load

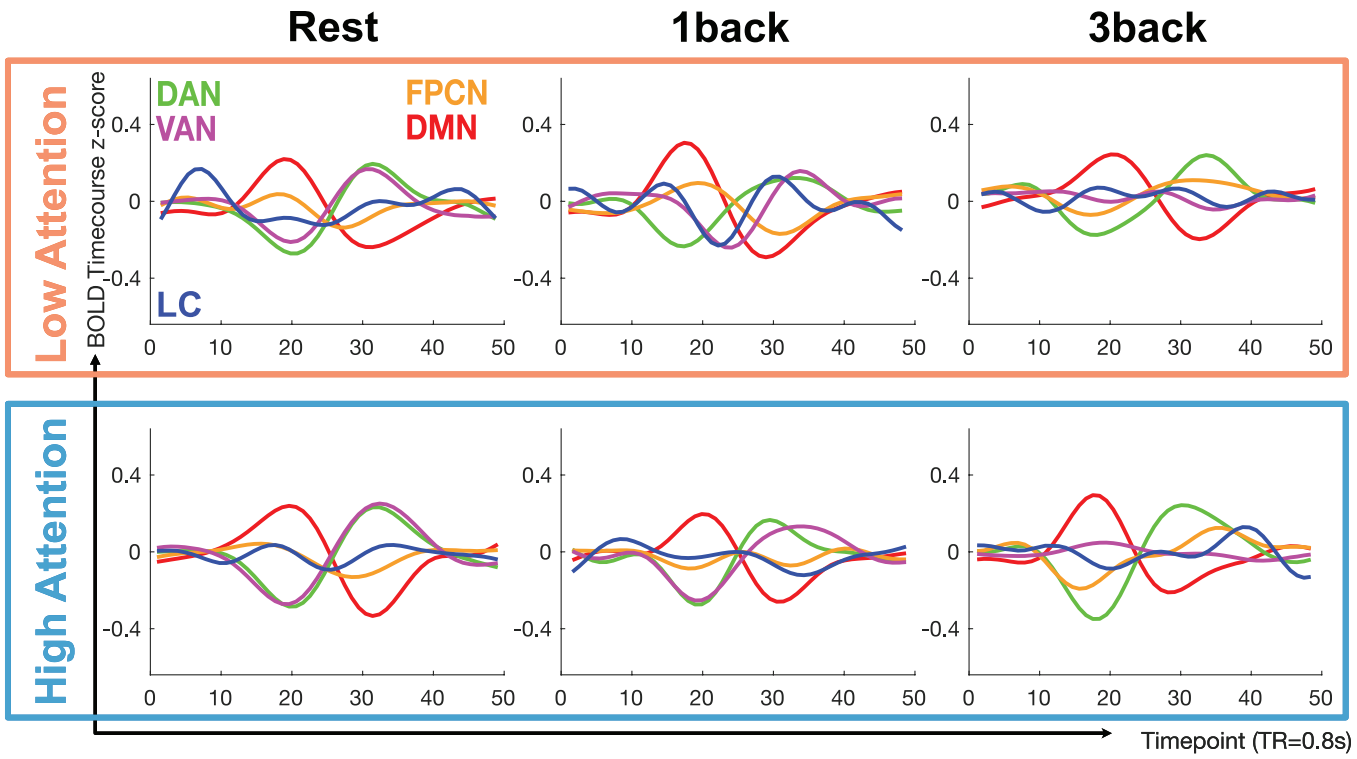

Fig. 3. Visualization of the QPP template results on the residualized attention control latent factor estimated score ($n = 30$) for high attention and ($n = 30$) for low attention. *FPCN* frontoparietal control network, *DMN* default mode network, *DAN* dorsal attention network, *VAN* ventral attention network, *LC* locus coeruleus.

condition, whereas individuals with higher attention control exhibited stronger reconfiguration only under high cognitive load.

This pattern was evident in FPCN interactions with the DMN. Individuals with lower attention control showed relatively strong positive FPCN–DMN coupling during rest that diminished substantially as task demands increased, indicating disengagement of internally oriented processing at low cognitive load. In contrast, individuals with higher attention control showed relatively little change between rest and low load but exhibited pronounced negative FPCN–DMN coupling under high load, suggesting stronger task-dependent segregation of internally directed processes when cognitive demands were greatest.

A similar load-dependent pattern was observed for FPCN interactions with attention-related networks. For the DAN, individuals with lower attention control showed larger connectivity shifts from rest to low cognitive load, whereas individuals with higher attention control exhibited the strongest increases in FPCN–DAN coupling under high cognitive load. This pattern suggests that individuals with higher attention control more strongly recruit goal-directed attention systems when task demands are greatest.

A more complex pattern emerged for interactions between the FPCN and the VAN. At rest, individuals with higher attention control exhibited a positive FPCN–VAN correlation that gradually decreased as cognitive load increased. In contrast, individuals with lower attention control showed a more variable pattern, shifting from negative coupling at rest to positive coupling under low load, and then returning to negative coupling under high load. This pattern aligns with a previous within-subject study (38), which found that during sustained "in-the-zone" states the FPCN decouples from the VAN while the VAN becomes more synchronized with the DMN.

Beyond cortico-cortical network interactions, trait differences in attention control were also reflected in how the LC, a neuromodulatory brainstem system, coordinated with the FPCN. Higher attention control individuals showed stronger positive coupling between the LC and the FPCN, specifically under high cognitive load. This configuration suggests coordination between the LC and FPCN, consistent with a more phasic LC mode (57) that enhances goal-directed engagement. The result aligns with animal work showing that LC firing (58, 59) increases with task difficulty and tracks behavioral response demands, and with human pupillometry showing that pupil dilation increases with cognitive effort and predicts performance (60). Given the LC's extensive noradrenergic projections and bidirectional interactions with the PFC, these findings suggest that trait-level attention control emerges not only from flexible coordination of large-scale brain networks, as proposed by Spreng et al. (39) but also the capacity to dynamically recruit the LC as cognitive load increases. Although traditionally linked to arousal, the LC likely plays a central role in supporting complex cognitive functions, including attention control, via modulation of FPCN dynamics.

These results provide direct fMRI evidence linking individual differences in attention control to LC function, supporting theoretical accounts that have largely relied on indirect or behavioral indices (45, 46). From these perspectives, individual differences in attention control stem in part from the efficiency with which the LC–norepinephrine system coordinates with large-scale networks as task demands increase.

These results may also reflect differences in how much cognitive effort individuals are willing or able to sustain as task demands increase. High attention control individuals may have continued to allocate effort and maintain engagement, whereas low attention control individuals may have reduced effort investment or partially disengaged when demands exceeded their ability to perform at a high level.

Despite high correlations among latent factors of attention control, working memory capacity, and fluid intelligence, we are confident that the QPP, which captures infraslow brain activity

via fMRI, reflects something distinctively related to attention control. Our multilevel modeling includes the residualized score of attention control independent of shared variance with working memory capacity and fluid intelligence; in other words, we isolate the contribution of attention control and still find significant interactions. This fits with accounts suggesting that attention control is a foundational mechanism underpinning both working memory capacity and fluid intelligence (1, 2, 9, 61, 62).

Taken together, these findings provide converging evidence that QPP-derived dynamics capture both state and trait-like neural signatures specific to attention control. While interrelated with working memory and fluid intelligence, attention control appears to leave a unique footprint in the brain's infraslow oscillations.

Implications

These findings bridge trait and state perspectives and advances our understanding of how cortical and neuromodulatory systems jointly support attention control. In addition, this highlights potential biomarkers of attentional control with direct relevance for mental health and applied performance contexts.

Limitations and Future Directions

Several limitations should be noted. The LC is small and anatomically variable, and our use of a standardized mask in MNI space introduces some imprecision; subject-specific neuromelanin images would provide greater accuracy. Second, global signal regression (GSR) remains controversial due to concerns that it may artificially induce anticorrelations or obscure meaningful global fluctuations. However, researchers (63) suggest that the global signal may obscure underlying neurophysiology and its removal can be useful. Future work could examine interindividual differences in the global signal characteristics—potentially offering another marker of trait-level differences. Third, while comparing 1-back and 3-back conditions gives us a window into state-level changes of brain dynamics, it is important to acknowledge that these tasks are not just harder or easier versions of the same task, as they likely engage different strategies altogether. Future research would benefit from a more adaptive task design, titrated to each participant's performance level, to more precisely capture how attention networks and the LC respond to increasing cognitive demands. In recent years, research has suggested that large-scale networks, including the FPCN (64), can be further subdivided into distinct subnetworks. Future studies may further characterize these networks to better understand their underlying functional nuances. Finally, the relationships we observed are correlational and should not be interpreted as causal without further investigation. Multiple fMRI sessions will be required to interrogate the stability of these dynamics across days and can strengthen the claim of trait-like nature of these signals. Furthermore, interventional work such as pharmacological modulation or noninvasive brain stimulation targeting the FPCN and LC would be valuable in testing whether changes in connectivity between these neural pathways actively supports attentional control or merely reflects it.

Conclusion

By combining latent-variable modeling, QPP analysis, and a large fMRI sample, this study identifies a dynamic neural signature of trait-level attention control. Stronger FPCN–DMN segregation, greater FPCN–DAN and FPCN–LC coupling, especially under high load, together provide a mechanistic account of why some individuals are better able to control their attention. Furthermore, these neural signatures were apparent during rest, indicating a possible task-ready state that high attention individuals may possess. This trait and state interaction underscores the dynamic nature of attentional processes in that state-level adaptations appear scaffolded by stable trait-level individual differences in neural organization.

Materials and Methods

Participants. Two hundred seventeen adults participated in a three-session study consisting of two behavioral sessions and one MRI session. Participants were between 18 and 35 y old, with strong right-handedness, no color-blindness, no history of seizures, no neurological issues, and were MRI safe. Recruitment included both college students (63.2%) and community members (36.9%). Compensation was scaled by session. Exclusions due to incomplete data ($n = 10$), structural anomalies ($n = 5$), excessive motion ($n = 3$), or missing behavioral results ($n = 3$) yielded a final sample of $N = 196$ (52% female; $M = 23.6$ y, $SD = 4.7$). The study was approved by the Institutional Review Boards of Georgia Institute of Technology (H22265 and H24045) and all participants provided written informed consent prior to participation.

Cognitive Measures. Latent factors of attention control, working memory capacity, and fluid intelligence were each assessed outside the fMRI scanner with multiple tasks on two separate days. Data were cleaned for chance performance and outliers. Confirmatory factor analysis (65) was used to extract the three factors, and scores were estimated for each individual using the Bartlett (66) method. Details of the tasks design and behavioral data processing are reported in *SI Appendix*.

fMRI Acquisition. MRI data were acquired on a 3 T Siemens Magnetom Prisma^{fit} MRI with a 32-channel head coil at GSU/GT Center for Advanced Brain Imaging, Atlanta. Field maps were collected at the start of each session. 3D T1-weighted MPRAGE and 3D T2-weighted SPACE scans were acquired at 0.8 mm^3 resolution. The task-fMRI and rest-fMRI scans were acquired using a multiband GRE-EPI sequence with the following parameters: 750 volumes, 72 slices, TR = 800 ms, TE = 37.40 ms, field of view = 208 × 208 mm, voxel dimensions = 2.0 × 2.0 × 2.0 mm, MB = 8. The order of these runs was counterbalanced in the study. Participants were instructed to keep their eyes open and focused on a fixation cross during the 10 min resting-state (no-load condition). The 1-back (low-load condition) and 3-back (high-load condition) tasks were based on the Human Connectome Project n-back protocol and were acquired separately with a duration of 10 min each. The participants practiced the n-back tasks prior to entering the MRI. Details of the task design are reported in *SI Appendix*.

Preprocessing. Data were preprocessed using the Configurable Pipeline for the Analysis of Connectomes (C-PAC) (67). Steps included bias correction, skull stripping, slice-timing and distortion correction, motion correction, MNI registration, nuisance regression (including white matter, cerebrospinal fluid, and GSR), temporal bandpass filtering (0.01 to 0.1 Hz), quadratic detrending, and spatial smoothing (4 mm FWHM). Following head motion guidelines (48), 5 participants with mean framewise displacement >0.12 mm and 40% of frames > 0.2 mm were excluded from the analysis. Finally, the scans were parcellated using the Schaefer2018 400-ROI, 7-network MNI152 parcellation (68) for the cortex, and the probabilistic MNI152 atlas (2 SD) by Keren et al. (69) was used to identify the LC while 3dROIstats was used to extract the BOLD signal.

QPP Analysis. A pattern-finding algorithm originally described by Majeed et al. (47) and further refined by others (56, 70) was applied separately to each participant's functional scan–resting state, 1-back, and 3-back. Each scan was 10 min (volumes = 750). The QPP detection algorithm can be summarized in these steps. First, it selects an initial spatiotemporal brain pattern of 20 s (timepoints = 25, TR = 800 ms) of each brain scan. Second, it uses a sliding window correlation to iteratively search across the scan for spatiotemporal patterns where the BOLD signal correlates, at a threshold of local maxima of $r = 0.2$, with the initial pattern. Third, as the correlating patterns are identified, they are averaged into the original pattern (updating the pattern as the search progresses). This process continues until the end of the brain scan. Steps 1 to 4 were repeated for all starting timepoints excluding the last 20 s within each participant. Last, the number of instances where the BOLD signal correlates above threshold for each different spatiotemporal pattern is calculated and ranked. The pattern with the highest sum occurrence is selected as the QPP template

for each functional scan for each participant. In this way, the algorithm identifies the most commonly repeating pattern of network activity for each subject and each task. Within this QPP template is where correlation time courses between the FPCN and DMN, DAN, VAN, and LC were extracted for each subject and load condition. A detailed process flowchart of the QPP analysis can be found in *SI Appendix*, figure S2 of Yousefi and Keilholz (56). The code for QPP analysis is openly available at https://github.com/imnanxu/QPPLab (70).

The QPP template visualization was generated from a high and low group split on the residualized (unique) estimate scores of attention control construct as a visual aid. The top, $n = 30$, ranking in each group served as the high attention control group while the bottom, $n = 30$ ranking served as the low attention control group and the QPP templates are averaged from the individual QPP templates which serves as the most common connectivity pattern for each group.

Statistical Analysis. Multilevel linear models were used to test whether FPCN connectivity within the QPP varied by trait-level attention control and load condition. To do so, the average BOLD signal of all the regions of interest (ROIs) from the FPCN was entered as a Level 1 predictor of another network/region of interest–DAN, DMN, VAN, and LC. The load conditions–rest, 1-back, and 3-back–were entered as Level 2. While Level 3 was the unresidualized (shared variance) or the residualized (unique variance) trait-level attention control, z-scored entered as a continuous variable. This setup answers the question of the unique contribution of attention control–independent of working memory capacity and fluid intelligence–to the QPP signal as a function of task demands. A stricter alpha threshold ($P < 0.01$) was used to correct for the multiple comparisons of tasks.

Data, Materials, and Software Availability. QPP time series and cognitive task scores data have been deposited in OSF https://osf.io/27yhq/ (71).

ACKNOWLEDGMENTS. This work was supported by the Office of Naval Research Grants N000142212218 and N000142312768 to R.W.E. We also thank the reviewers for their valuable time and feedback. Portions of this manuscript previously appeared as part of the PhD dissertation of author D.T.S.

Author affiliations: [a]School of Psychology, Georgia Institute of Technology, Atlanta, GA 30332; [b]Department of Psychology, University of North Carolina Wilmington, Wilmington, NC 28403; [c]Fischell Department of Bioengineering, University of Maryland, College Park, MD 20742; [d]Georgia State/Georgia Tech Center for Advanced Brain Imaging, Georgia Institute of Technology, Atlanta, GA 30332; and [e]Department of Biomedical Engineering, Emory University and Georgia Institute of Technology, Atlanta, GA 30332

1. A. P. Burgoyne, R. W. Engle, Attention control: A cornerstone of higher-order cognition. *Curr. Dir. Psychol. Sci.* **29**, 624–630 (2020).
2. R. W. Engle, Working memory and executive attention: A revisit. *Perspect. Psychol. Sci.* **13**, 190–193 (2018).
3. D. A. Norman, T. Shallice, "Attention to action: Willed and automatic control of behavior" in *Consciousness and Self-Regulation*, R. J. Davidson, G. E. Schwartz, D. Shapiro, Eds. (Springer, 1986), pp. 1–18.
4. M. M. Botvinick, T. S. Braver, D. M. Barch, C. S. Carter, J. D. Cohen, Conflict monitoring and cognitive control. *Psychol. Rev.* **108**, 624–652 (2001).
5. T. Egner, Congruency sequence effects and cognitive control. *Cogn. Affect. Behav. Neurosci.* **7**, 380–390 (2007).
6. A. Miyake *et al.*, The unity and diversity of executive functions and their contributions to complex "frontal lobe" tasks: A latent variable analysis. *Cogn. Psychol.* **41**, 49–100 (2000).
7. M. I. Posner, S. E. Petersen, The attention system of the human brain. *Annu. Rev. Neurosci.* **13**, 25–42 (1990).
8. R. W. Engle, "What is working memory capacity?" in *The Nature of Remembering: Essays in Honor of Robert G. Crowder*, H. L. Roediger III, J. S. Nairne, I. Neath, A. M. Surprenant, Eds. (American Psychological Association, 2001), pp. 297–314.
9. R. W. Engle, Working memory capacity as executive attention. *Curr. Dir. Psychol. Sci.* **11**, 19–23 (2002).
10. A. Baddeley, Exploring the central executive (1996).
11. E. Borella, B. Carretti, S. Pelegrina, The specific role of inhibition in reading comprehension in good and poor comprehenders. *J. Learn. Disabil.* **43**, 541–552 (2010).
12. T. Rohde, L. Thompson, Predicting academic achievement with cognitive ability. *Intelligence* **35**, 83–92 (2007).
13. F. Spinath, N. Harlaar, R. Plomin, Predicting school achievement from general cognitive ability, self-perceived ability, and intrinsic value. *Intelligence* **34**, 363–374 (2006).
14. J. A. Welsh, R. L. Nix, C. Blair, K. L. Bierman, N. E. Nelson, The development of cognitive skills and gains in academic school readiness for children from low-income families. *J. Educ. Psychol.* **102**, 43–53 (2010).
15. H. Miller, Self-control and health outcomes in a nationally representative sample. *Am. J. Health Behav.* **35**, 2 (2011).
16. A. Diamond, The evidence base for improving school outcomes by addressing the whole child and by addressing skills and attitudes, not just content. *Early Educ. Dev.* **21**, 780–793 (2010).
17. T. A. Judge, R. L. Klinger, L. S. Simon, Time is on my side: Time, general mental ability, human capital, and extrinsic career success. *J. Appl. Psychol.* **95**, 92–107 (2010).
18. T. S. Braver, M. W. Cole, T. Yarkoni, Vive les differences! Individual variation in neural mechanisms of executive control. *Curr. Opin. Neurobiol.* **20**, 242–250 (2010).
19. J. B. Keller *et al.*, Resting-state anticorrelations between medial and lateral prefrontal cortex: Association with working memory, aging, and individual differences. *Cortex* **64**, 271–280 (2015).
20. A. E. Reineberg, J. R. Andrews-Hanna, B. E. Depue, N. P. Friedman, M. T. Banich, Resting-state networks predict individual differences in common and specific aspects of executive function. *Neuroimage* **104**, 69–78 (2015).
21. M. Song *et al.*, Default network and intelligence difference. *IEEE Trans. Auton. Ment. Dev.* **1**, 101–109 (2009).
22. A. A. Stevens, S. C. Tappon, A. Garg, D. A. Fair, Functional brain network modularity captures inter- and intra-individual variation in working memory capacity. *PLoS One* **7**, 1–10 (2012).
23. M. P. van den Heuvel, C. J. Stam, R. S. Kahn, H. E. Hulshoff Pol, Efficiency of functional brain networks and intellectual performance. *J. Neurosci.* **29**, 7619–7624 (2009).
24. Z. Yuan *et al.*, The salience network contributes to an individual's fluid reasoning capacity. *Behav. Brain Res.* **229**, 384–390 (2012).
25. A. Kucyi *et al.*, Prediction of stimulus-independent and task-unrelated thought from functional brain networks. *Nat. Commun.* **12**, 1 (2021).
26. M. D. Rosenberg *et al.*, A neuromarker of sustained attention from whole-brain functional connectivity. *Nat. Neurosci.* **19**, 165–171 (2016).
27. E. K. Miller, J. D. Cohen, An integrative theory of prefrontal cortex function. *Annu. Rev. Neurosci.* **24**, 167–202 (2001).
28. M. J. Kane, R. W. Engle, The role of prefrontal cortex in working-memory capacity, executive attention, and general fluid intelligence: An individual-differences perspective. *Psychon. Bull. Rev.* **9**, 637–671 (2002).
29. M. Corbetta, G. L. Shulman, Control of goal-directed and stimulus-driven attention in the brain. *Nat. Rev. Neurosci.* **3**, 201–215 (2002).
30. R. N. Spreng, W. D. Stevens, J. P. Chamberlain, A. W. Gilmore, D. L. Schacter, Default network activity, coupled with the frontoparietal control network, supports goal-directed cognition. *Neuroimage* **53**, 303–317 (2010).
31. A. Fornito, B. J. Harrison, A. Zalesky, J. S. Simons, Competitive and cooperative dynamics of large-scale brain functional networks supporting recollection. *Proc. Natl. Acad. Sci. U.S.A.* **109**, 12788–12793 (2012).
32. P. J. Hellyer *et al.*, The control of global brain dynamics: Opposing actions of frontoparietal control and default mode networks on attention. *J. Neurosci.* **34**, 451–461 (2014).
33. M. D. Fox *et al.*, The human brain is intrinsically organized into dynamic, anticorrelated functional networks. *Proc. Natl. Acad. Sci. U.S.A.* **102**, 9673–9678 (2005).
34. M. E. Raichle, The brain's default mode network. *Annu. Rev. Neurosci.* **38**, 433–447 (2015).
35. W. W. Seeley *et al.*, Dissociable intrinsic connectivity networks for salience processing and executive control. *J. Neurosci.* **27**, 2349–2356 (2007).
36. V. Menon, L. Q. Uddin, Saliency, switching, attention and control: A network model of insula function. *Brain Struct. Funct.* **214**, 655–667 (2010).
37. S. M. Szczepanski, M. A. Pinsk, M. M. Douglas, S. Kastner, Y. B. Saalmann, Functional and structural architecture of the human dorsal frontoparietal attention network. *Proc. Natl. Acad. Sci. U.S.A.* **110**, 15806–15811 (2013).
38. T. Liebe, J. Kaufmann, D. Hämmerer, M. Betts, M. Walter, In vivo tractography of human locus coeruleus–Relation to 7T resting state fMRI, psychological measures and single subject validity. *Mol. Psychiatry* **27**, 4984–4993 (2022).
39. R. N. Spreng, J. Sepulcre, G. R. Turner, W. D. Stevens, D. L. Schacter, Intrinsic architecture underlying the relations among the default, dorsal attention, and frontoparietal control networks of the human brain. *J. Cogn. Neurosci.* **25**, 74–86 (2013).
40. A. F. T. Arnsten, P. S. Goldman-Rakic, Selective prefrontal cortical projections to the region of the locus coeruleus and raphe nuclei in the rhesus monkey. *Brain Res.* **306**, 9–18 (1984).
41. G. Aston-Jones, J. D. Cohen, An integrative theory of locus coeruleus-norepinephrine function: Adaptive gain and optimal performance. *Annu. Rev. Neurosci.* **28**, 403–450 (2005).
42. S. Bouret, S. J. Sara, Network reset: A simplified overarching theory of locus coeruleus noradrenaline function. *Trends Neurosci.* **28**, 574–582 (2005).
43. M. Corbetta, G. Patel, G. L. Shulman, The reorienting system of the human brain: From environment to theory of mind. *Neuron* **58**, 306–324 (2008).
44. J. M. Shine *et al.*, The dynamics of functional brain networks: Integrated network states during cognitive task performance. *Neuron* **92**, 544–554 (2016).
45. N. Unsworth, M. K. Robison, A locus coeruleus-norepinephrine account of individual differences in working memory capacity and attention control. *Psychon. Bull. Rev.* **24**, 1281–1311 (2017).
46. J. S. Tsukahara, R. W. Engle, Fluid intelligence and the locus coeruleus–norepinephrine system. *Proc. Natl. Acad. Sci. U.S.A.* **118**, e2110630118 (2021).
47. W. Majeed *et al.*, Spatiotemporal dynamics of low frequency BOLD fluctuations in rats and humans. *Neuroimage* **54**, 1140–1150 (2011).
48. B. Yousefi, J. Shin, E. H. Schumacher, S. D. Keilholz, Quasi-periodic patterns of intrinsic brain activity in individuals and their relationship to global signal. *Neuroimage* **167**, 297–308 (2018).
49. A. Abbas *et al.*, Quasi-periodic patterns contribute to functional connectivity in the brain. *Neuroimage* **191**, 193–204 (2019).
50. A. M. C. Kelly, L. Q. Uddin, B. B. Biswal, F. X. Castellanos, M. P. Milham, Competition between functional brain networks mediates behavioral variability. *Neuroimage* **39**, 527–537 (2008).
51. G. J. Thompson *et al.*, Short-time windows of correlation between large-scale functional brain networks predict vigilance intraindividually and interindividually. *Hum. Brain Mapp.* **34**, 3280–3298 (2013).
52. A. Kucyi, M. J. Hove, M. Esterman, R. M. Hutchison, E. M. Valera, Dynamic brain network correlates of spontaneous fluctuations in attention. *Cereb. Cortex* **27**, 1831–1840 (2017).

53. R. Esposito *et al.*, Modifications in resting state functional anticorrelation between default mode network and dorsal attention network: Comparison among young adults, healthy elders and mild cognitive impairment patients. *Brain Imaging Behav.* **12**, 127–141 (2018).
54. D. T. Seeburger *et al.*, Time-varying functional connectivity predicts fluctuations in sustained attention in a serial tapping task. *Cogn. Affect. Behav. Neurosci.* **24**, 111–125 (2024).
55. A. Abbas, Y. Bassil, S. Keilholz, Quasi-periodic patterns of brain activity in individuals with attention-deficit/hyperactivity disorder. *Neuroimage Clin.* **21**, 101653 (2019).
56. B. Yousefi, S. Keilholz, Propagating patterns of intrinsic activity along macroscale gradients coordinate functional connections across the whole brain. *Neuroimage* **231**, 117827 (2021).
57. E. Durán, M. Yang, R. Neves, N. K. Logothetis, O. Eschenko, Modulation of prefrontal cortex slow oscillations by phasic activation of the locus coeruleus. *Neuroscience* **453**, 268–279 (2021).
58. J. Rajkowski, H. Majczynski, E. Clayton, G. Aston-Jones, Activation of monkey locus coeruleus neurons varies with difficulty and performance in a target detection task. *J. Neurophysiol.* **92**, 361–371 (2004).
59. P. Bornert, S. Bouret, Locus coeruleus neurons encode the subjective difficulty of triggering and executing actions. *PLoS Biol.* **19**, e3001487 (2021).
60. P. Van der Wel, H. Van Steenbergen, Pupil dilation as an index of effort in cognitive control tasks: A review. *Psychon. Bull. Rev.* **25**, 2005–2015 (2018).
61. C. Draheim, T. L. Harrison, S. E. Embretson, R. W. Engle, What item response theory can tell us about the complex span tasks. *Psychol. Assess.* **30**, 116–129 (2018).
62. C. A. Mashburn, J. S. Tsukahara, R. W. Engle, "Individual differences in attention control" in *Working Memory: The State of the Science*, R. H. Logie, V. Camos, N. Cowan, Eds. (Oxford University Press, 2020), pp. 175–211.
63. M. D. Fox, D. Zhang, A. Z. Snyder, M. E. Raichle, The global signal and observed anticorrelated resting state brain networks. *J. Neurophysiol.* **101**, 3270–3283 (2009).
64. M. L. Dixon *et al.*, Heterogeneity within the frontoparietal control network and its relationship to the default and dorsal attention networks. *Proc. Natl. Acad. Sci. U.S.A.* **115**, E1598–E1607 (2018).
65. Y. Rosseel, lavaan: An R package for structural equation modeling. *J. Stat. Softw.* **48**, 1–36 (2012).
66. M. S. Bartlett, The statistical conception of mental factors. *Br. J. Psychol.* **28**, 97–104 (1937).
67. C. Craddock *et al.*, Towards automated analysis of connectomes: The configurable pipeline for the analysis of connectomes (c-pac). *Front. Neuroinform. Conf. Proc: Neuroinformatics* (2013). https://internal-www.frontiersin.org/10.3389/conf.fninf.2013.09.00042/event_abstract.
68. A. Schaefer *et al.*, Local-global parcellation of the human cerebral cortex from intrinsic functional connectivity MRI. *Cereb. Cortex* **28**, 3095–3114 (2018).
69. N. I. Keren, C. T. Lozar, K. C. Harris, P. S. Morgan, M. A. Eckert, In vivo mapping of the human locus coeruleus. *Neuroimage* **47**, 1261–1267 (2009).
70. N. Xu *et al.*, QPPLab: A generally applicable software package for detecting, analyzing, and visualizing large-scale quasiperiodic spatiotemporal patterns (QPPs) of brain activity. *SoftwareX* **29**, 102067 (2025).
71. D. T. Seeburger, J. S. Tsukahara, R. W. Engle, Attention control ability is associated with frontoparietal control network interactions. Open Science Framework. https://osf.io/27yhq/. Accessed 20 April 2026.